# Computational probes of molecular motion in the Lewis-Wahnström model for *ortho*-terphenyl

Thomas G. Lombardo and Pablo G. Debenedetti[a)]
*Department of Chemical Engineering, Princeton University, Princeton, New Jersey 08544*

Frank H. Stillinger
*Department of Chemistry, Princeton University, Princeton, New Jersey 08544*

We use molecular dynamics simulations to investigate translational and rotational diffusion in a rigid three-site model of the fragile glass former *ortho*-terphenyl, at 260 K $\leq T \leq$ 346 K and ambient pressure. An Einstein formulation of rotational motion is presented, which supplements the commonly used Debye model. The latter is shown to break down at supercooled temperatures as the mechanism of molecular reorientation changes from small random steps to large infrequent orientational jumps. We find that the model system exhibits non-Gaussian behavior in translational and rotational motion, which strengthens upon supercooling. Examination of particle mobility reveals spatially heterogeneous dynamics in translation and rotation, with a strong spatial correlation between translationally and rotationally mobile particles. Application of the Einstein formalism to the analysis of translation-rotation decoupling results in a trend opposite to that seen in conventional approaches based on the Debye formalism, namely, an enhancement in the effective rate of rotational motion relative to translation upon supercooling. © *2006 American Institute of Physics.*
[DOI: 10.1063/1.2371111]

## I. INTRODUCTION

Molecular motion in supercooled liquids has received much scrutiny from experiments and simulations in recent years.[1,2] These studies have uncovered a rich phenomenology not present at temperatures above the melting point. One distinguishing feature is commonly known as dynamic heterogeneity. This refers to the presence of transient spatially separated regions with vastly different relaxation times.[1] Observed in experiments[3–5] and simulations,[6–10] these domains are separated by only a few nanometers but can differ by up to five orders of magnitude in their rate of relaxation.[1] Closely related to dynamic heterogeneity is a non-Gaussian distribution of particle displacements at times intermediate between the ballistic and diffusive regimes of molecular motion.[8] This behavior is a common aspect of supercooled liquids and has been used extensively to detect dynamic heterogeneity in computer simulations.[6,8] Dynamic heterogeneity has also been invoked to explain the decoupling between translational diffusion and viscosity and between rotational and translational diffusion in deeply supercooled liquids.[1,11,12] At $T \gtrsim 1.2T_g$, where $T_g$ is the glass transition temperature, the translational diffusion coefficient $D_t$ and the rotational diffusion coefficient $D_r$ are proportional to $T\eta^{-1}$, where $\eta$ is the shear viscosity. This is in accord with the Stokes-Einstein (SE) equation for translational diffusion,

$$D_t = \frac{k_B T}{6\pi \eta R}, \tag{1}$$

and its rotational counterpart, the Debye-Stokes-Einstein (DSE) relation,

$$D_r = \frac{k_B T}{8\pi \eta R^3}. \tag{2}$$

In both expressions $k_B$ is Boltzmann's constant and $R$ is an effective hydrodynamic radius of the diffusing particle. The fact that these equations, which describe diffusion of a Brownian particle in a hydrodynamic continuum with viscosity $\eta$, apply at the molecular scale is remarkable. Yet, as liquids enter the deeply supercooled regime, $T \lesssim 1.2T_g$, experiments suggest that the SE equation (e.g., Refs. 13 and 14) and perhaps also the DSE equation (e.g., Refs. 15–19) break down. Experiments on *ortho*-terphenyl (1,2-diphenylbenzene, OTP) reveal that $D_t$ is approximately proportional to $T\eta^{-0.8}$ in this regime and that the SE equation underpredicts $D_t$ by as much as two orders of magnitude at $T_g + 3$ K.[13,14,20] Studies on rotational motion in OTP are less conclusive on the validity of the DSE equation in this temperature range. Some studies have upheld the DSE equation down to $T_g$,[13,14] while others have shown $D_r$ to be proportional to $(T/\eta)^{\xi}$ with $\xi \leq 1$ at $T \lesssim 1.2T_g$.[15–19,21]

The goal of the present work is to investigate numerically the diffusive phenomena in a model supercooled liquid. Special emphasis is placed on rotational motion, an important aspect of supercooled liquid dynamics that has received comparatively less attention than its translational counterpart in existing investigations of dynamic heterogeneity and non-Gaussian behavior. Examples of recent studies of rotational

---

[a)]Electronic mail: pdebene@princeton.edu

**125**, 174507-1

dynamics in supercooled liquids include Refs. 22–26. Inclusion of rotational degrees of freedom provides the means to study computationally translation-rotation decoupling, a phenomenon observed experimentally in many fragile glass formers. To investigate these topics we perform molecular dynamics simulations of the rigid three-site Lewis-Wahnström model of OTP (Ref. 27) at temperatures spanning the warm thermodynamically stable liquid to deeply supercooled states.

This paper is organized as follows. Section II provides the background on the two formalisms used here to characterize rotational diffusion; Section III extends metrics for dynamic heterogeneity and non-Gaussian behavior of translational motion to rotation. Section IV presents the results obtained from molecular dynamics simulations of OTP and discusses their significance. The major conclusions arrived at in this work and the open questions arising as a result of our study are listed in Sec. V.

## II. ROTATIONAL FORMALISM

The most common framework for exploring rotational motion originates with the work of Debye.[28] The underlying physical picture views rotational diffusion as a succession of small, random processes. A unit vector fixed to the center of mass of a rotating molecule would then undergo a random walk on the surface of a sphere. Solving the differential equation for the evolution of the probability $P(\psi,t)$ that a molecule experiences a net angular displacement $\psi$ during a time $t$ then yields[29]

$$P(\psi,t) = \sum_{l=1}^{\infty} \left( \frac{2l+1}{2} \right) P_l[\cos\psi] e^{-l(l+1)D_r t}. \quad (3)$$

Here $P_l$ is the $l$th Legendre polynomial and $D_r$ is the rotational diffusion coefficient, with units of inverse time. The angular displacement is defined as $\psi(t) = \cos^{-1}[\mathbf{u}(t) \cdot \mathbf{u}(0)]$, where $\mathbf{u}$ is the unit vector fixed in the molecular frame. The first two Legendre polynomials, $l=1$ and $l=2$, can be related to several experimental techniques including infrared absorption, Raman scattering, and NMR.[30] These experiments often report rotational correlation times, $\tau_l = [l(l+1)D_r]^{-1}$, in place of a diffusion coefficient. These are straightforwardly calculated from

$$\tau_l = \int_0^{\infty} \langle P_l[\cos\psi(t)] \rangle dt. \quad (4)$$

At low temperatures, $P_l[\cos\psi(t)]$ decays slowly and long simulations are needed to reach the time necessary to accurately determine $\tau_l$ from Eq. (4). One may derive an equivalent relation from Eq. (3) and obtain a rotational correlation time from

$$\tau_l^{-1} = -\frac{d}{dt} \ln\langle P_l[\cos\psi(t)] \rangle \quad (5)$$

in the region where $\ln\langle P_l[\cos\psi(t)] \rangle$ is linear in time. We have verified that Eqs. (4) and (5) give similar values of $\tau_l$ at high temperature where $P_l[\cos\psi(t)]$ decays quickly. We refer to this formulation of rotational motion as the Debye model.

The Debye model is well suited for examining the rotation of dipoles and diatomic or other rigid linear molecules because these systems provide a natural choice for the unit vector $\mathbf{u}$. However, in molecules with more than two rotational degrees of freedom (any rigid nonlinear molecule), at least two orthogonal unit vectors are required for a full description of rotational motion. As will be shown below, rotational motion along different directions can exhibit widely differing characteristics at low enough temperatures. Additionally, the Debye model has limited utility in examining dynamic heterogeneity and non-Gaussian behavior because the angular displacement $\psi$ is bounded between 0 and $\pi$. As will be shown in Sec. III, not only is an unbounded displacement critical to studying dynamic heterogeneity but also rotational motion in the deeply supercooled regime deviates appreciably, at least for the Lewis-Wahnström model considered here, from the physical picture of small uncorrelated angular displacements underlying the Debye model. In light of these facts, the following alternative rotational formalism is introduced. An angular displacement may be obtained in a manner analogous to that of translational displacement by integrating the angular velocity vector,[31]

$$\Delta\boldsymbol{\varphi}_i(t) = \boldsymbol{\varphi}_i(t) - \boldsymbol{\varphi}_i(0) = \int_0^t \boldsymbol{\omega}_i(t')dt'. \quad (6)$$

Here, $\boldsymbol{\omega}_i$ and $\Delta\boldsymbol{\varphi}_i$ are the angular velocity and angular displacement vectors for particle $i$, respectively. Note that $\Delta\boldsymbol{\varphi}_i$ is unbounded. For a generic rigid body with three rotational degrees of freedom, each component describes rotation about a specific principal axis fixed in the molecular frame and originating at the center of mass. The components are denoted by $\boldsymbol{\omega}_i = [\omega_i^x, \omega_i^y, \omega_i^z]$ and $\Delta\boldsymbol{\varphi}_i = [\Delta\varphi_i^x, \Delta\varphi_i^y, \Delta\varphi_i^z]$.

In this approach, rotational motion is anisotropic; each direction describes a specific rotational movement of the molecule. Associated with each rotational direction is a principal moment of inertia. These in general are not equivalent, and it is therefore appropriate to define diffusion coefficients for each degree of freedom, rather than for the molecule as a whole. As a starting point, consider the Einstein relation for the translational diffusion coefficient $D_t$ in one dimension,

$$D_t = \lim_{t\to\infty} \frac{1}{2tN} \sum_{i=1}^{N} \langle [\Delta x_i(t)]^2 \rangle. \quad (7)$$

Here $\Delta x_i(t)$ is the displacement of particle $i$ in the $x$ direction at time $t$, and the sum is over all molecules. A rotational diffusion coefficient in the $\varphi^\alpha$ direction, $D_r^\alpha$, can be defined analogously as

$$D_r^\alpha = \lim_{t\to\infty} \frac{1}{2tN} \sum_{i=1}^{N} \langle [\Delta\varphi_i^\alpha(t)]^2 \rangle, \quad (8)$$

where $\alpha \in [x, y, z]$. We refer to this description of rotational motion as the Einstein formulation, but note that in the rotational case the directions $\varphi^x$, $\varphi^y$, and $\varphi^z$ are in the molecular frame. An interesting feature of this formulation is that by appropriately selecting the orientational axes fixed in the molecular frame, the different diffusion coefficients will correspond to specific changes in orientation of the molecule. The
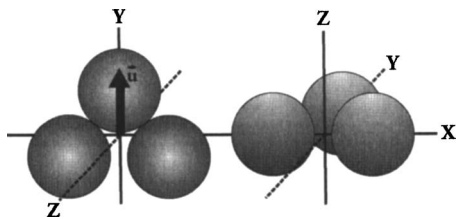
FIG. 1. Illustration of rotational directions in the Lewis-Wahnström model of OTP. In this model each phenyl ring is represented by a Lennard-Jones site, and the three sites constitute a rigid isosceles triangle with a vertex angle of 75° (Ref. 27). The unit vector (**u**) used here to study rotation according to the Debye model is also shown.

axes chosen in this paper are illustrated in Fig. 1.

Each of the above models of rotational motion has its advantages. The Debye model forms the basis of several experimental techniques (primarily via measurements of $P_2[\cos \psi(t)]$) and has therefore played an important role in studies of translation-rotation decoupling.[13,14,20,32] In contrast, the Einstein formulation has only been used in simulations,[23,26,31,33,34] but as will be shown below, it offers important advantages for the numerical investigation of dynamics in deeply supercooled liquids, where the physical basis of the Debye approximation appears to break down.

## III. NON-GAUSSIAN METRICS AND DYNAMIC HETEROGENEITY

The notion of dynamic heterogeneity implies the existence of a time scale intermediate between the ballistic and diffusive regimes over which particles of like mobility are spatially correlated. Therefore, in order to study dynamic heterogeneity, one must quantify "mobility" and identify this time scale. Most studies have defined mobility starting from the individual particle displacement vector $\Delta \mathbf{r}_i(\Delta t)$ and its associated scalar quantity $\Delta r_i(\Delta t)$. To facilitate comparison between translational and rotational diffusion and to connect with a recently developed diffusion formalism,[35] we elect to utilize the Cartesian component of the displacement vector, $\Delta x_i(\Delta t)$, for translation (the $y$ and $z$ directions are equivalent and are included as independent samples in all our calculations), and the individual angular displacements $\Delta \varphi_i^\alpha(\Delta t)$, for rotation, as the quantities of interest.

The work of Kob *et al.*[8] revealed that the dynamic heterogeneity of translational motion observed in computer simulations of a binary glass former is associated with a non-Gaussian probability distribution of particle displacements. For short times displacement may be approximated by $\Delta x_i \approx v_i^x \Delta t$ resulting in a probability distribution that is Gaussian due to the Maxwell-Boltzmann distribution of velocities,

$$P(\Delta x_i) \cong \sqrt{\frac{m}{2\pi k_B T(\Delta t)^2}} \exp\left(\frac{-m(\Delta x_i)^2}{2k_B T(\Delta t)^2}\right). \quad (9)$$

Also, at sufficiently long times, diffusion is purely random and the displacement distribution asymptotically adopts a Gaussian form,

$$P(\Delta x_i) \sim \frac{1}{2(\pi D_t \Delta t)^{1/2}} \exp\left(\frac{-(\Delta x_i)^2}{4D_t \Delta t}\right). \quad (10)$$

At intermediate times where these approximations are invalid, the behavior of $P(\Delta x_i)$ has been shown to be substantially non-Gaussian, reaching a maximum deviation from the Gaussian form at a time to be denoted by $\Delta t^*$. This time serves as the appropriate time scale on which to study dynamic heterogeneity of translational motion and corresponds approximately to the beginning of the long-time diffusive regime.

The extension of this idea to rotational motion is straightforward. At short times angular displacement may be approximated by $\Delta \varphi_i^\alpha \approx \omega_i^\alpha \Delta t$ and the probability distribution of angular displacements is accordingly Gaussian due to the Maxwell-Boltzmann distribution of angular velocities,

$$P(\Delta \varphi_i^\alpha) \cong \sqrt{\frac{I_\alpha}{2\pi k_B T(\Delta t)^2}} \exp\left(\frac{-I_\alpha (\Delta \varphi_i^\alpha)^2}{2k_B T(\Delta t)^2}\right). \quad (11)$$

Here $I_\alpha$ is the moment of inertia for a rotation in the $\varphi^\alpha$ direction with $\alpha \in [x, y, z]$. In analogy to translation, the distribution of angular displacements also converges to a Gaussian form at long times,

$$P(\Delta \varphi_i^\alpha) \sim \frac{1}{2(\pi D_r^\alpha \Delta t)^{1/2}} \exp\left(\frac{-(\Delta \varphi_i^\alpha)^2}{4D_r^\alpha \Delta t}\right). \quad (12)$$

Similarly to translation, we will show that at times intermediate between these approximations $P(\Delta \varphi_i^\alpha)$ is non-Gaussian, and we will focus on the time of maximum non-Gaussian behavior $\Delta t^*$. We use this time to examine dynamic heterogeneity of rotational motion. The notation $\Delta t^*$ is used here generically, and we will see that $\Delta t^*$ for translation is not in general the same as $\Delta t^*$ for rotation.

Determination of $\Delta t^*$ requires an appropriate metric of non-Gaussian behavior. This is commonly done by using the ratio of the second and fourth moments of the appropriate probability distribution of particle displacement.[36] A useful non-Gaussian parameter is

$$\alpha_2^t(\Delta t) = \frac{\langle [\Delta x(\Delta t)]^4 \rangle}{5 \langle [\Delta x(\Delta t)^2] \rangle^2} - \frac{3}{5} \quad (13)$$

for translation and

$$\alpha_2^r(\Delta t) = \frac{\langle [\Delta \varphi^\alpha(\Delta t)^4] \rangle}{5 \langle [\Delta \varphi^\alpha(\Delta t)^2] \rangle^2} - \frac{3}{5} \quad (14)$$

for rotation. Each parameter is defined such that Gaussian behavior yields $\alpha_2^t = \alpha_2^r = 0$. This can be easily verified from Eqs. (10) and (12). The time at which $\alpha_2^t$ and $\alpha_2^r$ reach their maximum value identifies $\Delta t^*$ for translation and rotation, respectively.

Having specified a time scale $\Delta t^*$, particles may be classified as "mobile" and "immobile" using an appropriate displacement cutoff. Objective specification of this cutoff is challenging and previous studies have explored several options. We elect to use a method developed by Shell *et al.*[6] which defines a displacement cutoff that can be easily adapted to the rotational formalism used here. This technique fits a two-Gaussian function of the form

TABLE I. Diffusion coefficients at each investigated temperature and density for translation and rotation as measured via the Einstein model and the second Legendre polynomial.

| $T$ (K) | $\rho$ (g/cm$^3$) | $D_t$ ($10^{-5}$ cm$^2$/s) | $D_r^x$ (ns$^{-1}$) | $D_r^y$ (ns$^{-1}$) | $D_r^z$ (ns$^{-1}$) | $D_r$ ($P_2$) (ns$^{-1}$) |
|---|---|---|---|---|---|---|
| 346 | 1.027 | 0.23 | 7.6 | 3.7 | 3.6 | 4.0 |
| 305 | 1.055 | 0.057 | 2.3 | 1.3 | 1.3 | 1.0 |
| 291 | 1.065 | 0.023 | 0.95 | 0.51 | 0.58 | 0.38 |
| 275 | 1.076 | 0.0072 | 0.42 | 0.29 | 0.35 | 0.12 |
| 266 | 1.079 | 0.0018 | 0.18 | 0.16 | 0.24 | 0.024 |
| 260 | 1.082 | 0.0013 | 0.14 | 0.15 | 0.18 | 0.014 |

$$P(z) = fG(z;\sigma_1) + (1-f)G(z;\sigma_2) \qquad (15)$$

to the probability distribution of displacements at the time $\Delta t^*$. Here $f$ is a weighting parameter with $0 \leq f \leq 1$, $G(z;\sigma)$ is a Gaussian distribution in $z$ with zero mean and standard deviation $\sigma$, and $z$ signifies $\Delta x$ or $\Delta \varphi^\alpha$. This functional form reproduces the measured distribution at $\Delta t^*$ well with only a slight underestimation of the tails. The standard deviations of the two-Gaussian fit differ by a factor of 1.5–2.5 and are an objective measure of the displacement of mobile and immobile particles. These values are used to define cutoff values and segregate particles into mobile and immobile groups. This method has the advantage of using objective length scales to classify mobility as opposed to specifying an arbitrary percentage of particles to be mobile and immobile. For translation, a reasonable three-dimensional cutoff is $\Delta r^* = \sqrt{3}(\sigma_1+\sigma_2)/2$ (Ref. [6]). The $\sqrt{3}$ factor accounts for calculation of the standard deviations from a one-dimensional probability distribution, since $\langle[\Delta r]^2\rangle = 3\langle[\Delta x]^2\rangle$. For each rotational direction, a one-dimensional cutoff is defined as $\Delta \varphi^{\alpha*} = (\sigma_1+\sigma_2)/2$. Particles are classified as translationally mobile if $\Delta r_i(\Delta t^*) > \Delta r^*$ and rotationally mobile in the $\varphi^\alpha$ direction if $\Delta \varphi_i^\alpha(\Delta t^*) > \Delta \varphi^{\alpha*}$.

## IV. SIMULATION RESULTS AND DISCUSSION

We have performed molecular dynamics simulations of the Lewis-Wahnström model for OTP.[27] In this model each benzene ring is represented by a single Lennard-Jones (LJ) site on a rigid isosceles triangle. The two short sides of the triangle are one LJ diameter, $\sigma$, in length (0.483 nm), and the long side is 1.217 LJ diameters long (0.588 nm), giving a vertex angle of 75°. The sites on different molecules interact pairwise additively with a LJ interaction energy of $\epsilon/k_B = 600$ K. The chosen directions of the molecular frame give $I_x:I_y:I_z = 1:1.77:2.77$. Calculation runs are performed in the $NVE$ ensemble for $N=324$ molecules (972 LJ sites) at a range of temperatures of 260 K $\leq T \leq$ 346 K. The density at each temperature is given in Table I and corresponds to the equilibrium density for the model at 1 bar as determined by Rinaldi et al.[37] With the exception of quantities reported in Table I, all values are reported in reduced units with the mass of an OTP molecule, characteristic interaction energy $\epsilon$, and atomic diameter $\sigma$ as the reference units. The reduced time unit is then 3.19 ps. The rigid body equations of motion were integrated using a half-step leap-frog Verlet scheme[38] for translation and an iterative quaternion algorithm[39] for rota-

tion with a step size of 0.001 reduced time units. To improve statistics, multiple time origins separated by 0.1–0.3 reduced time units were employed in the calculations that follow.

The mean square displacement (MSD) is shown in Fig. 2 for one-dimensional translation (the $x$, $y$, and $z$ directions are equivalent and used as independent samples) and rotation in each of three molecular frame directions (see Fig. 1). As in previous studies[7,26,31] we observe three distinct regimes for both translational and rotational displacements. Molecular motion is initially ballistic with MSD proportional to $(\Delta t)^2$. Following this initial period is a plateau corresponding to the entrapment of molecules in the cage formed by their neighbors. Towards the end of the plateau, the non-Gaussian parameter attains its maximum value and thereafter the long-time diffusive regime begins, as evidenced by the emerging proportionality between the MSD and $\Delta t$. The diffusion coefficients for translation and rotation are determined from the slope of the MSD in this region and are listed in Table I. An interesting feature that emerges from Table I is the relative value of $D_r$ between the different rotational directions. At warm temperatures, the rotational diffusion coefficients are ordered in accordance with their associated moments of inertia (i.e., $D_r^x > D_r^y > D_r^z$, consistent with $I_x < I_y < I_z$). This trend gradually reverses itself such that at 260 K, the diffusion coefficients obey $D_r^x < D_r^y < D_r^z$. It seems plausible that this may be the result of the increasing importance of steric hindrance upon cooling. A rotation in the $\varphi^z$ direction (see Fig. 1) is a rotation of the plane of the OTP model and is sterically easier than rotations in the $\varphi^x$ and $\varphi^y$ directions. Additionally, the effect of steric hindrance may be amplified by the increase in density that results from cooling at constant pressure. Further work is needed to substantiate this interpretation.

The behavior of the non-Gaussian parameter over the range of temperatures investigated here is shown in Fig. 3 for translation and each of the rotational directions. As the model OTP is cooled, $\Delta t^*$ increases and corresponds approximately to the transition from the cage to the long-time diffusive regime at each temperature. For $T > 291$ K, $\Delta t^*$ is approximately coincident for translation and rotation. However, for $T < 291$ K, $\Delta t^*(T)$ increases rapidly with decreasing temperature for translation, such that at $T=260$ K, $\Delta t^*$ is an order of magnitude larger for translation than for any rotational direction. Two interesting results are shown in Figs. 2 and 3. The first is the difference in maximum $\alpha_2^r$ values between the $\varphi^x$ and the $\varphi^y$ and $\varphi^z$ directions. The non-Gaussian
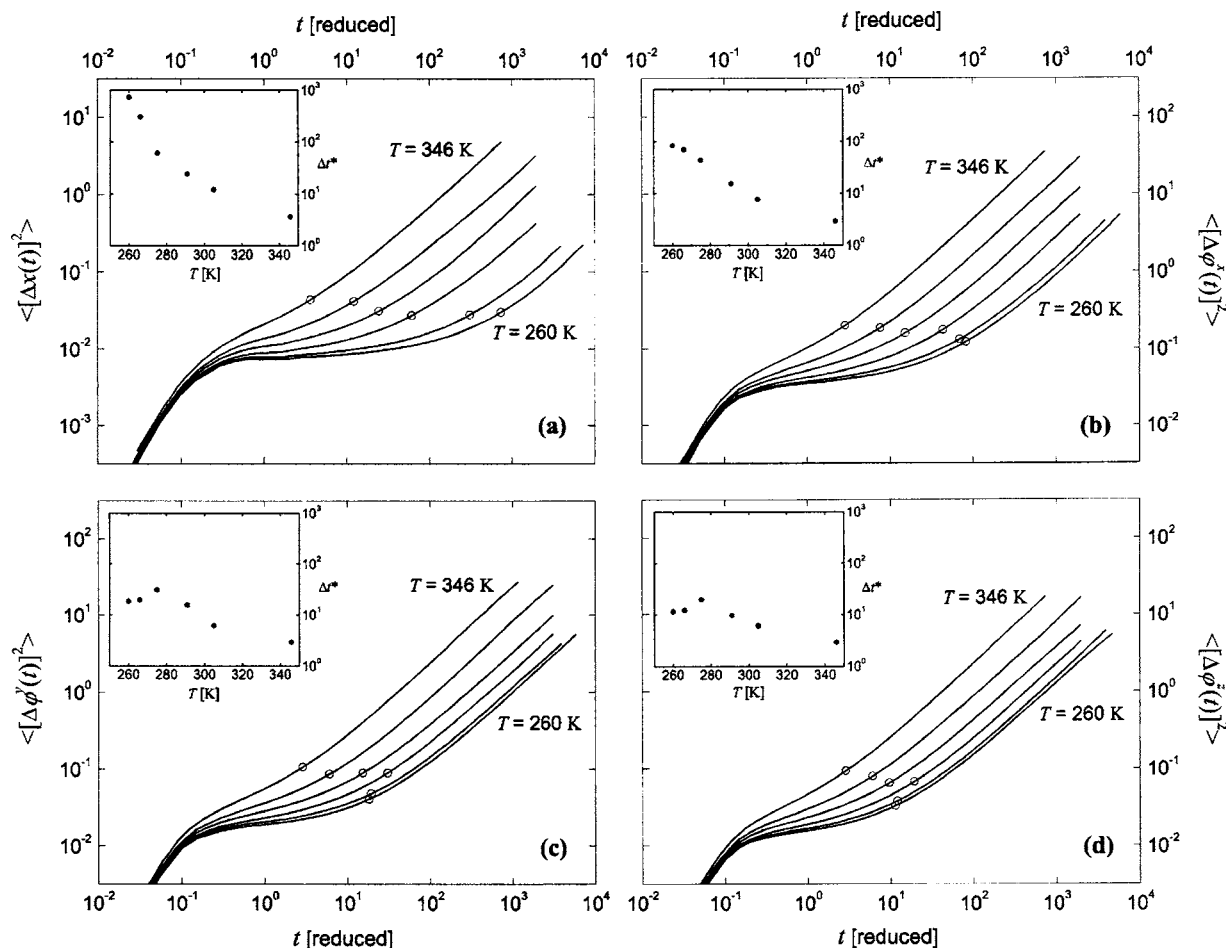
FIG. 2. Mean square displacement at $T=260$, 266, 275, 291, 305, and 346 K for (a) translation in one dimension and (b) rotation in the $\varphi^x$, (c) $\varphi^y$, and (d) $\varphi^z$ directions with temperature increasing from bottom to top. The time of maximum non-Gaussian behavior, $\Delta t^*$, is marked with an open circle on each plot and shown as a function of temperature in the inset plot for each direction.

parameter in the $\varphi^x$ direction reaches a maximum value of approximately 1.7, while $\alpha_2^r$ in the $\varphi^y$ and $\varphi^z$ directions does not exceed 0.5. The second feature of note is the nonmonotonic behavior of $\Delta t^*(T)$ and $\alpha_2^r(\Delta t^*)$ in the $\varphi^y$ and $\varphi^z$ directions. After an initial increase upon cooling down to 275 K, $\Delta t^*(T)$ and $\alpha_2^r(\Delta t^*)$ begin to decrease as the temperature decreases. This trend continues down to the lowest temperature studied. In contrast, a recent study of SPC/E water[26] showed all rotational directions to be qualitatively similar, with $\Delta t^*(T)$ and $\alpha_2^r(\Delta t^*)$ monotonically increasing as temperature decreases. We have verified that these results are not an artifact of cooling at constant pressure as opposed to constant density, by performing a subset of isochoric runs and comparing the behavior of the non-Gaussian parameter.

A complementary approach to the study of non-Gaussian behavior is based on a recently proposed alternative view of self-diffusion.[35] Integration of the velocity autocorrelation function leads to the following expressions:

$$D_t = \lim_{t \to \infty} \frac{1}{3} \langle \mathbf{v}(0) \cdot \Delta \mathbf{r}(t) \rangle, \tag{16}$$

$$D_r^\alpha = \lim_{t \to \infty} \langle \omega^\alpha(0) \Delta \varphi^\alpha(t) \rangle. \tag{17}$$

The physical interpretation of these equations is that the diffusion constant is a measure of the extent to which initial

velocity biases long-time displacement. Equations (16) and (17) can be written more formally as an integral of a joint probability distribution of initial velocity and final displacement,[6]

$$D_t = \lim_{\Delta t \to \infty} \int \int v_0^x \Delta x P(v_0^x, \Delta x) dv_0^x d\Delta x, \tag{18}$$

$$D_r^\alpha = \lim_{\Delta t \to \infty} \int \int \omega_0^\alpha \Delta \varphi^\alpha P(\omega_0^\alpha, \Delta \varphi^\alpha) d\omega_0^\alpha d\Delta \varphi^\alpha. \tag{19}$$

Here $P(v_0^x, \Delta x)$ and $P(\omega_0^\alpha, \Delta \varphi^\alpha)$ are the joint probability distributions of initial velocity and eventual displacement, and the isotropy of translational motion allows the replacement of $P(\mathbf{v}_0, \Delta \mathbf{r})$ with a factor of three times the distribution of one-dimensional displacement, $P(v_0^x, \Delta x)$. The necessary probability distributions are easily calculated from a molecular dynamics simulation by maintaining a two-dimensional histogram of initial velocity and displacement after a specified time $\Delta t$.

Figure 4 shows contour plots of the joint probability distributions at short, intermediate, and long times at 275 K. At short times, initial velocity and displacement are highly correlated, resulting in a distribution that is skewed along $\Delta x = v_0^x \Delta t$ and $\Delta \varphi^\alpha = \omega_0^\alpha \Delta t$. Interactions with other molecules soon weaken this correlation, and the distribution accord-
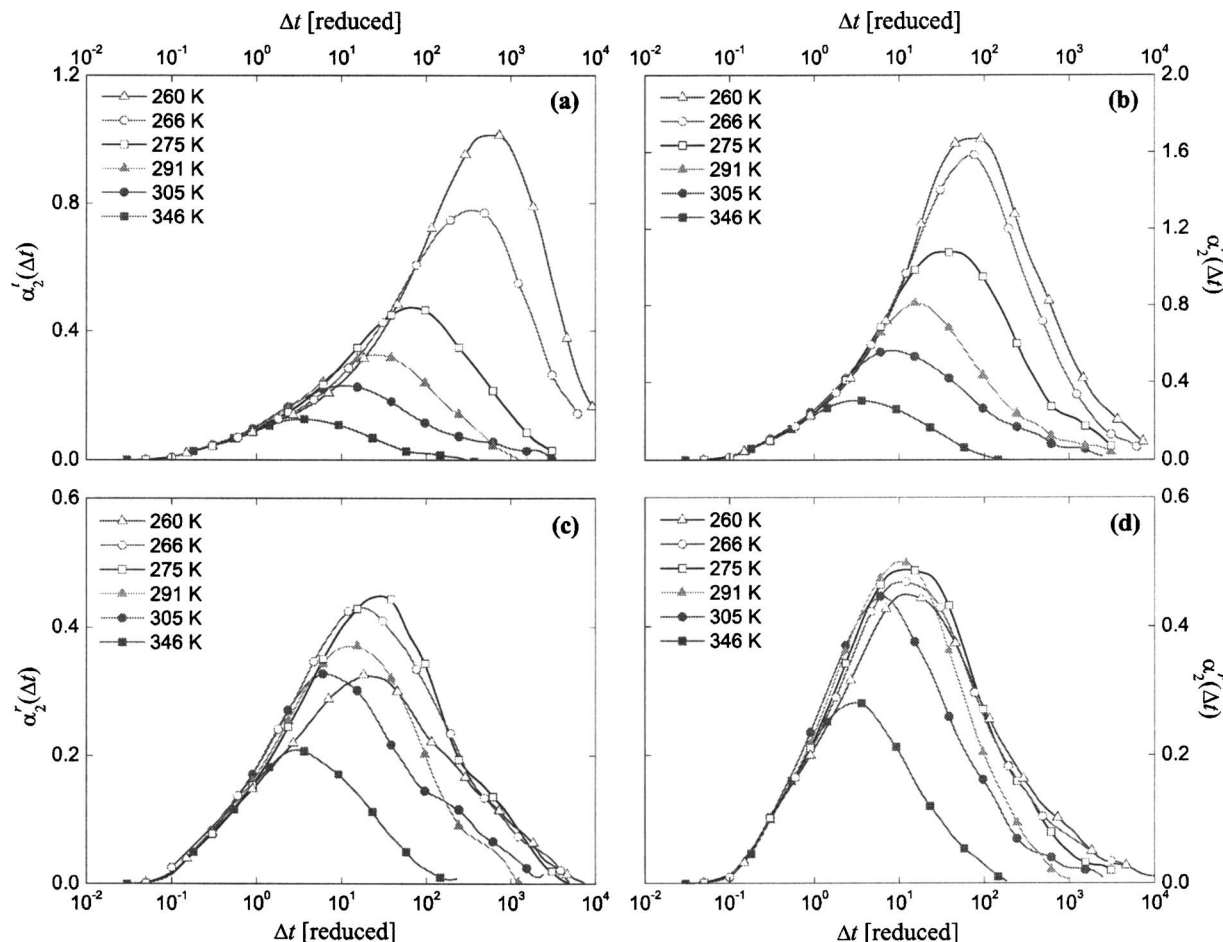
FIG. 3. The non-Gaussian parameters, $\alpha_2^t$ and $\alpha_2^r$, for (a) translation in one dimension and (b) rotation in the $\varphi^x$, (c) $\varphi^y$, and (d) $\varphi^z$ directions. The time at which $\alpha_2^t$ and $\alpha_2^r$ attain their maximum value corresponds to $\Delta t^*$.

ingly appears axisymmetric, with circular contours clearly visible. However, when the joint probability distribution is evaluated at $\Delta t = \Delta t^*$, it develops a distinct "diamond distortion." This behavior was first reported for translational motion by Shell *et al.* for a binary mixture of Lennard-Jones particles[40] but has not previously been reported for rotational motion. This distinctive shape may be reproduced by the combination of a Maxwell-Boltzmann distribution of velocities and a two-Gaussian distribution of particle displacements in the form of Eq. (15). Random diffusive motion eventually returns the distributions to a single Gaussian shape at long times. We have calculated $P(v_0^x, \Delta x)$ and $P(\omega_0^\alpha, \Delta \varphi^\alpha)$ at all investigated temperatures and for several time scales in addition to those shown in Fig. 4. Over this range of conditions we find that the time of maximum diamond distortion corresponds approximately to $\Delta t^*$. In addition the relative strength of the distortion is consistent with the values of $\alpha_2^t$ and $\alpha_2^r$. Namely, the contour plots become increasingly "diamond" shaped at $\Delta t^*$ as the temperature is reduced with the exception of the few instances in the $\varphi^y$ and $\varphi^z$ directions when a decrease in temperature leads to decrease in the maximum value of $\alpha_2^r$.

The diamond distortion of the joint probability histograms evaluated at $\Delta t^*$ reveals interesting information about molecular motion. The circular shape of the contours at short and long times is a result of the Gaussian nature of the par-

ticle displacement probability distribution, since the velocities obey the Gaussian Maxwell-Boltzmann distribution at all times. At intermediate times, characterized by $\Delta t^*$, the tails of the measured probability distribution of particle displacements are significantly increased relative to a single Gaussian distribution with zero mean and estimated standard deviation, thus causing the diamond distortion.[6] By computing $\alpha_2^t$ and $\alpha_2^r$ for various initial velocities, we found that non-Gaussian behavior is uniform across all initial velocities (both translational and angular) once the regime of ballistic particle motion has ended, after approximately 0.4 reduced time units. This is consistent with the behavior reported in Ref. 6 for an atomic system and confirms that the distinctive diamond distortion is entirely due to non-Gaussian behavior of particle displacements and is unrelated to the initial velocity distribution.

To detect the presence of spatially heterogeneous dynamics, we have computed the pair correlation function for the centers of mass of mobile molecules at 260 K, as shown in Fig. 5. To compute these correlations, molecules are classified into mobile and immobile groups for translation and each rotational direction based on the criteria presented in Sec. III. However, the different values of $\Delta t^*$ for translation and the three rotational directions complicate this process. To allow the calculation of correlations that involve more than a single direction, such as correlations between translation and
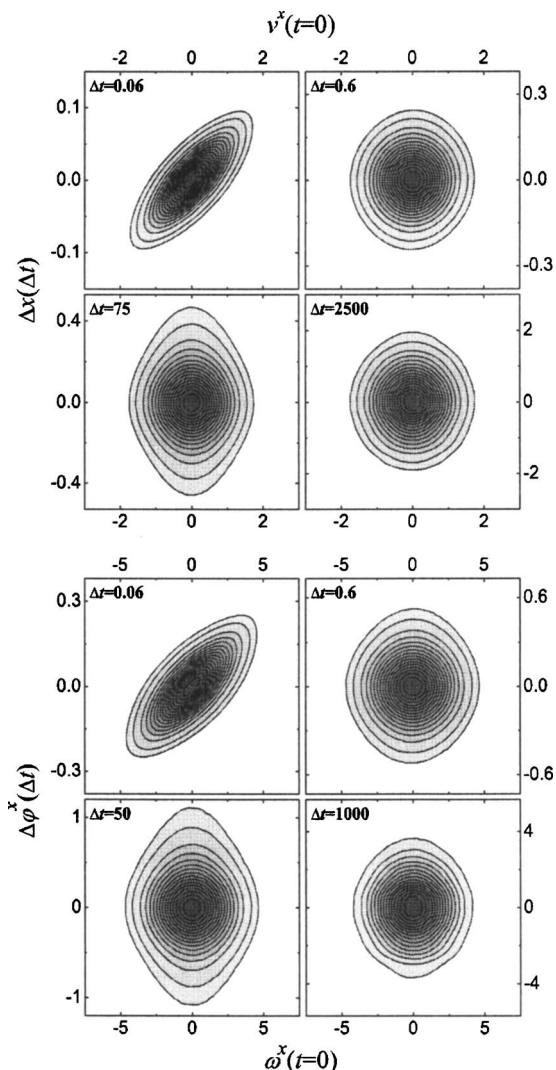
FIG. 4. Contour plots of the joint probability distributions of initial velocity and displacement after a time $\Delta t$ for (top) translation and (bottom) rotation in $\varphi^x$ at 275 K. The various values of $\Delta t$ are marked on each plot. The $\varphi^y$ and $\varphi^z$ directions behave similarly to the $\varphi^x$ plots shown.
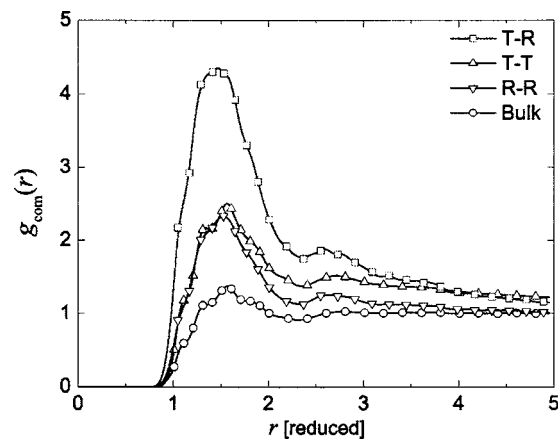


FIG. 5. Pair correlation function for the centers of mass of mobile molecules as defined in Sec. III at 260 K. T-T designates the correlation between pairs of translationally mobile molecules, while R-R is the rotational counterpart with pairs of molecules simultaneously mobile in $\varphi^x$, $\varphi^y$, and $\varphi^z$. T-R represents the correlation between molecules that are mobile concurrently in translation and all rotational directions.

rotation or between more than a single rotational direction, molecules are classified as mobile or immobile based on their future displacement. This procedure begins by selecting a particle configuration and then examining translational and angular displacements after the appropriate time $\Delta t^*$ for each direction has elapsed. Molecules are then classified as mobile or immobile in each direction, and pair correlation functions are generated from the initial particle configuration by examining center of mass pairwise correlations as a function of distance between molecules that are appropriately classified. This process is then repeated over many time origins to improve statistics. Figure 5 shows enhanced correlations between molecules that are translationally mobile and between molecules that are rotationally mobile. However, the rotational correlation is only significantly increased when it is restricted to molecules that are mobile in all rotational directions (i.e., molecules that are simultaneously mobile in $\varphi^x$, $\varphi^y$, and $\varphi^z$). These enhanced correlations indicate that the dynamics of the Lewis-Wahnström model for OTP is spatially heterogeneous in both translation and rotation. In addi-

tion, the cross correlation between translationally and rotationally mobile molecules (i.e., molecules that are simultaneously mobile in translation and all rotational directions) shows the strong tendency for these molecules to be in close proximity. These results are similar to a recent computational study of water, which found a strong similarity between translational and rotational heterogeneities.[26]

The Debye model leads to experimentally accessible measures of rotation, and many studies of supercooled liquids, including simulations, accordingly rely on it. Most of these examinations obtain rotational diffusion coefficients from the decay of the second Legendre polynomial and Eq. (4). Figure 6 shows the evolution of the ensemble-averaged second Legendre polynomial calculated for the Lewis-Wahnström model of OTP at each of the temperatures investigated. At lower temperatures a two-step relaxation process is evident, as seen from the initial short-time decrease, which is followed by a long-time tail. We examined $P_1$ through $P_5$ but only show $P_2$ because of its experimental significance. In theory, one may use any of the Legendre polynomials to compute $D_r$ using Eq. (5) and $D_r = [l(l+1)\tau_l]^{-1}$ and should
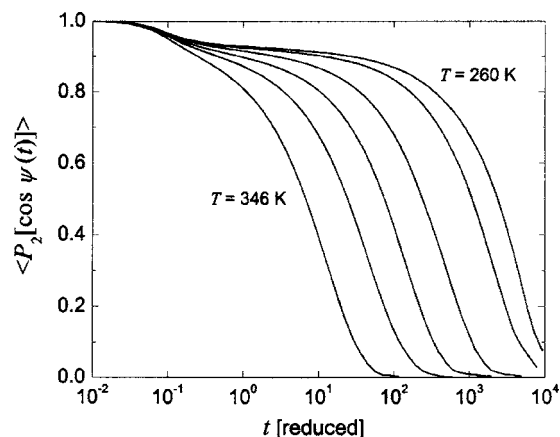


FIG. 6. Time dependence of the second Legendre polynomial at $T=260$, 266, 275, 291, 305, and 346 K. The unit vector **u** used in this calculation is shown in Fig. 1. Temperature decreases moving from left to right.

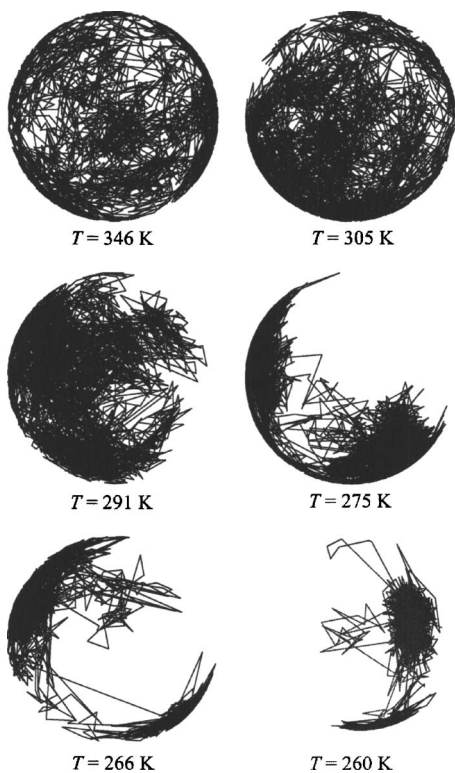FIG. 7. Single-molecule rotational trajectory of the unit vector **u** (see Fig. 1), employed in the Debye model of rotation at each investigated temperature. The total time for each trajectory is the time necessary for $\langle \cos \psi(t) \rangle$ to decay to 0.05.
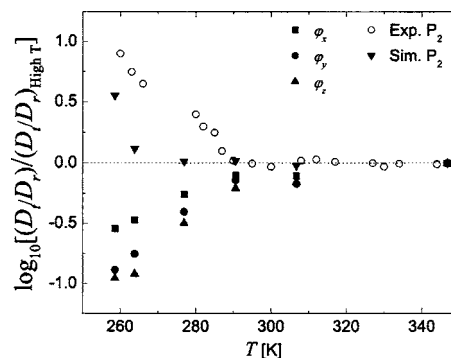


FIG. 8. Temperature dependence of the logarithm of the ratio of translational to rotational diffusion coefficients normalized by the corresponding value at high temperatures. Experimental data are from Refs. 13 and 20.

obtain the same result. However, we find that $D_r$ decreases as the order of the Legendre polynomial is increased [i.e., $D_r(P_1) > D_r(P_2) > D_r(P_3)$ and so on]. In addition, the Debye model predicts that the ratio of rotational correlation times measured from the first and second Legendre polynomials, $\tau_1/\tau_2$, should be equal to 3. We find that this ratio decreases from 2.45 at 346 K down to 1.60 at 260 K. Deviation from this theoretical value in supercooled liquids is associated with long angular jumps.[23,41] Such behavior was shown to be prominent in this model at 266 K by Lewis and Wahnström.[27,42]

In addition to the Legendre polynomials, an informative representation of the validity of the Debye model is the single-molecule trajectory of the vector **u** on a unit sphere over the time required for $\langle \cos \psi(t) \rangle$ to decay to a small value.[34] Figure 7 shows representative trajectories for all investigated temperatures. At 346 K, **u** explores uniformly the entire surface of the unit sphere in a manner that is consistent with the Debye approximation (i.e., small random steps). Upon supercooling, the trajectory of **u** no longer covers the whole surface and becomes trapped in small regions of the sphere surface over extended periods of time. This behavior is characteristic of a change in the mechanism of reorientation from consistently small random steps to well-separated and sudden changes of orientation. In this new mechanism molecules undergo librational movement for a significant amount of time before jumping to a new orientation. This type of movement is clearly visible in the trajectory of **u** at 266 and 260 K. Figure 7 vividly shows a breakdown of Debye behavior.

One of the distinctive aspects of supercooled liquid behavior is the decoupling of translational and rotational motion.[2] There is considerable interest in exploring the microscopic basis of this behavior, with most studies focusing on the breakdown of the Stokes-Einstein (SE) and the possible breakdown of the Debye-Stokes-Einstein (DSE) relations [see Eqs. (1) and (2), respectively]. Relevant studies of this picture include experimental,[13–20] theoretical,[11,12,43,44] and computational investigations.[21,45] A convenient metric of translation-rotation decoupling is the quotient $D_t/D_r$ normalized by the same quantity at high temperature[12,20] (one may equivalently use $D_t \tau_l$ in place of $D_t/D_r$). Figure 8 shows this quantity as a function of temperature, using diffusion coefficients obtained at 346 K as the high-temperature reference values. Included in this figure are rotational diffusion coefficients based on the Debye model obtained from $\langle P_2[\cos \psi(t)] \rangle$, as well as the three rotational coefficients resulting from the Einstein formulation. Figure 8 also includes experimental rotational correlation times calculated from deuteron spin alignment ($^2$H-NMR) experiments using Eq. (4) with $l=2$ (Refs. 13 and 46) and experimental translational diffusion coefficients from a recent study by Mapes et al.[20]

Figure 8 reveals a significant result. Upon entering the deeply supercooled regime, experiments and simulations that measure rotation using the Debye model display a significant increase in $D_t/D_r$ as temperature decreases. This is in accord with the traditional concept of translation-rotation decoupling, indicating an increase in the effective translational diffusion coefficient relative to its rotational counterpart (i.e., the system behaves effectively as if, upon cooling, molecules translate further for every rotation they execute). However, when $D_r$ is calculated from the Einstein formulation, Eq. (8), $D_t/D_r$ decreases as the temperature decreases, indicating an effective increase in the rate of rotational diffusion relative to translation. This suggests the need for a critical reexamination of our current understanding of translation-rotation decoupling in supercooled liquids, especially in light of its dependence on the Debye model.

## V. CONCLUDING REMARKS

The diversity and complexity of dynamic phenomena present in supercooled liquids are a major challenge to a comprehensive understanding of this important class of

condensed-phase systems. Computer simulation is an important tool that provides insight into the details of molecular motion in a manner that is not currently possible in experiments. To further the understanding of diffusion in supercooled liquids, we have studied a model of the canonical fragile glass former *ortho*-terphenyl. In particular, we have extended the formalism and techniques developed for studying dynamic heterogeneity in translational motion[6,35] to a molecular system with rotational degrees of freedom. These methods revealed spatially heterogeneous dynamics in translation and rotation with a strong spatial correlation between the translationally and rotationally mobile molecules. The commonly used Debye model of rotation was shown to break down at deeply supercooled temperatures, as the mechanism for molecular reorientation begins to incorporate large angular jumps. When the Einstein formulation of rotational motion was used to examine translation-rotation decoupling, the analysis showed a trend opposite to that observed when using the Debye model to quantify rotational diffusion. Specifically, the effective rate of rotational motion appears to be enhanced relative to translation. This result, coupled with the concurrent breakdown of the Debye model, calls into question conventional interpretations of the relationship between translational and rotational motion in deeply supercooled liquids.

Models that explain translation-rotation decoupling are based on the picture provided by dynamic heterogeneity[11,12,47] and rely on the Debye model to describe rotation. By assuming the presence of regions of fast and slow dynamics, translation-rotation decoupling emerges as temperature falls below some critical value (e.g., $T \lesssim 1.2 T_g$) as a consequence of the different ways in which translational and rotational motion are averaged in regions of slow and fast dynamics.[11] In this view, the SE and DSE equations are assumed to be obeyed locally in both the slow and fast regions of the dynamically heterogeneous liquid.[3] It can then be shown that the effective translational diffusion coefficient is given approximately by $(D_t^s + D_t^f)/2$, where the superscripts $s$ and $f$ denote the slow and fast regions, respectively, and it is assumed in this approximate calculation that the slow and fast regions each accounts for half of the system's volume.[3] Using similar arguments, the rotational correlation time is given by $(\tau_l^s + \tau_l^f)/2$. Thus, the translational diffusion coefficient is determined by the dynamics of the fast regions, whereas the rotational correlation time is determined by the dynamics of the slow regions.[1] A corresponding microscopic interpretation of the results shown in Fig. 8 when the Einstein formalism of rotation is used has yet to be developed. In particular, an understanding of how heterogeneity affects averaging in such a way as to produce an effective enhancement of rotation upon cooling needs to be developed.

An interesting question arising from our work is the origin of the nonmonotonic behavior of $\Delta t^*$ and $\alpha_2^r(\Delta t^*)$ in the $\varphi^y$ and $\varphi^z$ directions [see Figs. 2 and 3]. It is possible that this behavior may be caused by the onset of orientational hopping in the $\varphi^y$ and $\varphi^z$ directions. Future work will focus on the onset of orientational hopping in the various directions and, in particular, will test the eventual appearance of hopping in the $\varphi^x$ direction.

This and previous studies of the Lewis-Wahnström model for OTP suggest that its behavior differs from that of real OTP at supercooled temperatures. Its primary fault is the inaccurate prediction of diffusion coefficients. Our study and others[27,37] report diffusion coefficients that are three orders of magnitude larger for translation and seven orders of magnitude larger for rotation than experiments near 260 K indicate. This may in part result from fitting the Lennard-Jones interaction parameters to experimental values for the translational diffusion coefficient and molar volume at 400 K (Ref. 27) as opposed to a lower temperature. This change could be made with relative ease but raises the question of which molecular features of OTP contribute most to its glass-forming ability. OTP is known to interact with short-range van der Waals forces,[48] and the molecular structure exhibits some internal torsioning. These features have been incorporated into other models for OTP, including two 3-ring, 18-site Lennard-Jones molecules,[49,50] which retain some internal motions in the form of side ring torsions and vibrations. A third OTP model uses fully atomistic force field methods to describe the interactions.[51] While more accurate, these models are significantly more complex than the Lewis-Wahnström model, making it computationally challenging to use the system sizes and reach the simulation times necessary at deeply supercooled temperatures. The prominence of OTP as one of the most extensively studied fragile glass formers attests to the importance of developing an accurate model that captures the salient features of real OTP but is simple enough for use in simulation studies at supercooled temperatures. The Lewis-Wahnström model is a first step towards this goal, but improvements are warranted.

Our present analysis suggests further questions regarding the nature of dynamic heterogeneity. An important open question is how regions of high mobility emerge in the liquid. It is not yet understood what local properties of the liquid cause the molecules in these domains to have a high mobility. An interesting method to explore this question was introduced by Widmer-Cooper *et al.*[52–54] This technique involves running separate simulations from a single starting configuration. At the beginning of each run the momenta of each particle are randomly chosen from the appropriate Maxwell-Boltzmann distribution. Their results indicate that a particle's local environment, and not its initial velocity, has a strong effect on its propensity for motion. This suggests the existence of structural features that influence particle mobility and engender dynamic heterogeneity. It would be interesting to extend a study of this nature to include rotational degrees of freedom. The Einstein rotational formalism used in this paper lends itself well for such a study. Knowledge of the origin of dynamic heterogeneity would be a significant advance in the understanding of supercooled liquids.

## ACKNOWLEDGMENTS

[1] M. D. Ediger, Annu. Rev. Phys. Chem. **51**, 99 (2000).

[2] P. G. Debenedetti and F. H. Stillinger, Nature (London) **410**, 259 (2001).

[3] M. T. Cicerone and M. D. Ediger, J. Chem. Phys. **104**, 7210 (1996).

[4] M. D. Ediger, J. Phys. Chem. **100**, 13200 (1996).

[5] E. V. Russell and N. E. Israeloff, Nature (London) **408**, 695 (2000).

[6] M. S. Shell, P. G. Debenedetti, and F. H. Stillinger, J. Phys.: Condens. Matter **17**, S4035 (2005).

[7] N. Giovambattista, M. G. Mazza, S. V. Buldyrev, F. W. Starr, and H. E. Stanley, J. Phys. Chem. B **108**, 6655 (2004).

[8] W. Kob, C. Donati, S. J. Plimpton, P. H. Poole, and S. C. Glotzer, Phys. Rev. Lett. **79**, 2827 (1997).

[9] S. C. Glotzer, J. Non-Cryst. Solids **274**, 342 (2000).

[10] R. Richert, J. Phys.: Condens. Matter **14**, R703 (2002).

[11] F. H. Stillinger and J. A. Hodgdon, Phys. Rev. E **50**, 2064 (1994).

[12] G. Tarjus and D. Kivelson, J. Chem. Phys. **103**, 3071 (1995).

[13] F. Fujara, B. Geil, H. Sillescu, and G. Fleischer, Z. Phys. B: Condens. Matter **88**, 195 (1992).

[14] I. Chang, F. Fujara, B. Geil, G. Heuberger, T. Mangel, and H. Sillescu, J. Non-Cryst. Solids **172**, 248 (1994).

[15] L. Andreozzi, A. DiSchino, M. Giordano, and D. Leporini, Europhys. Lett. **38**, 669 (1997).

[16] L. Andreozzi, A. DiSchino, M. Giordano, and D. Leporini, J. Phys.: Condens. Matter **8**, 9605 (1996).

[17] L. Andreozzi, M. Faetti, and M. Giordano, J. Phys.: Condens. Matter **18**, 931 (2006).

[18] S. H. Bielowka, T. Psurek, J. Ziolo, and M. Paluch, Phys. Rev. E **63**, 062301 (2001).

[19] I. Chang and H. Sillescu, J. Phys. Chem. B **101**, 8794 (1997).

[20] M. K. Mapes, S. F. Swallen, and M. D. Ediger, J. Phys. Chem. B **110**, 507 (2006).

[21] S. R. Becker, P. H. Poole, and F. W. Starr, Phys. Rev. Lett. **97**, 055901 (2006).

[22] P. Sindzingre and M. L. Klein, J. Chem. Phys. **96**, 4681 (1992).

[23] C. De Michele and D. Leporini, Phys. Rev. E **63**, 036702 (2001).

[24] J. Kim, W. X. Li, and T. Keyes, Phys. Rev. E **67**, 021506 (2003).

[25] J. Kim and T. Keyes, J. Chem. Phys. **121**, 4237 (2004).

[26] M. G. Mazza, N. Giovambattista, F. W. Starr, and H. E. Stanley, Phys. Rev. Lett. **96**, 057803 (2006).

[27] L. J. Lewis and G. Wahnström, Phys. Rev. E **50**, 3865 (1994).

[28] P. Debye, *Polar Molecules* (Dover, New York, 1929).

[29] D. A. McQuarrie, *Statistical Mechanics* (Harper & Row, New York, 1975).

[30] J. P. Hansen and I. R. McDonald, *Theory of Simple Liquids* (Academic, London, 1986).

[31] S. Kammerer, W. Kob, and R. Schilling, Phys. Rev. E **56**, 5450 (1997).

[32] T. Dries, F. Fujara, M. Kiebel, E. Rossler, and H. Sillescu, J. Chem. Phys. **88**, 2139 (1988).

[33] S. Kammerer, W. Kob, and R. Schilling, Phys. Rev. E **58**, 2141 (1998).

[34] P. P. Jose, D. Chakrabarti, and B. Bagchi, Phys. Rev. E **71**, 030701(R) (2005).

[35] F. H. Stillinger and P. G. Debenedetti, J. Phys. Chem. B **109**, 6604 (2005).

[36] A. Rahman, Phys. Rev. A **136**, A405 (1964).

[37] A. Rinaldi, F. Sciortino, and P. Tartaglia, Phys. Rev. E **63**, 061210 (2001).

[38] M. P. Allen and D. J. Tildesley, *Computer Simulation of Liquids* (Clarendon, Oxford/Oxford University Press, New York, 1987).

[39] I. P. Omelyan, Phys. Rev. E **58**, 1169 (1998).

[40] M. S. Shell, P. G. Debenedetti, and F. H. Stillinger, J. Phys. Chem. B **109**, 21329 (2005).

[41] D. Kivelson and S. A. Kivelson, J. Chem. Phys. **90**, 4464 (1989).

[42] L. J. Lewis and G. Wahnström, J. Non-Cryst. Solids **172**, 69 (1994).

[43] J. A. Hodgdon and F. H. Stillinger, Phys. Rev. E **48**, 207 (1993).

[44] Y. J. Jung, J. P. Garrahan, and D. Chandler, Phys. Rev. E **69**, 061205 (2004).

[45] S. K. Kumar, G. Szamel, and J. F. Douglas, J. Chem. Phys. **124**, 214501 (2006).

[46] H. W. Spiess, J. Chem. Phys. **72**, 6755 (1980).

[47] M. T. Cicerone, P. A. Wagner, and M. D. Ediger, J. Phys. Chem. B **101**, 8727 (1997).

[48] J. D. Cox and R. J. L. Andon, Trans. Faraday Soc. **54**, 1622 (1958).

[49] S. R. Kudchadkar and J. M. Wiest, J. Chem. Phys. **103**, 8566 (1995).

[50] S. Mossa, R. Di Leonardo, G. Ruocco, and M. Sampoli, Phys. Rev. E **62**, 612 (2000).

[51] R. J. Berry, D. Rigby, D. Duan, and M. Schwartz, J. Phys. Chem. A **110**, 13 (2006).

[52] A. Widmer-Cooper, P. Harrowell, and H. Fynewever, Phys. Rev. Lett. **93**, 135701 (2004).

[53] A. Widmer-Cooper and P. Harrowell, J. Phys.: Condens. Matter **17**, S4025 (2005).

[54] A. Widmer-Cooper and P. Harrowell, Phys. Rev. Lett. **96**, 185701 (2006).